



This is a repository copy of *13.9% efficiency ternary nonfullerene organic solar cells featuring low-structural order*.

White Rose Research Online URL for this paper:
<http://eprints.whiterose.ac.uk/156045/>

Version: Supplemental Material

Article:

Du, B., Geng, R., Li, W. et al. (11 more authors) (2019) 13.9% efficiency ternary nonfullerene organic solar cells featuring low-structural order. *ACS Energy Letters*, 4 (10). pp. 2378-2385. ISSN 2380-8195

<https://doi.org/10.1021/acsenergylett.9b01630>

This document is the Accepted Manuscript version of a Published Work that appeared in final form in *ACS Energy Letters*, copyright © American Chemical Society after peer review and technical editing by the publisher. To access the final edited and published work see <https://doi.org/10.1021/acsenergylett.9b01630>

Reuse

Items deposited in White Rose Research Online are protected by copyright, with all rights reserved unless indicated otherwise. They may be downloaded and/or printed for private study, or other acts as permitted by national copyright laws. The publisher or other rights holders may allow further reproduction and re-use of the full text version. This is indicated by the licence information on the White Rose Research Online record for the item.

Takedown

If you consider content in White Rose Research Online to be in breach of UK law, please notify us by emailing eprints@whiterose.ac.uk including the URL of the record and the reason for the withdrawal request.



eprints@whiterose.ac.uk
<https://eprints.whiterose.ac.uk/>

Supporting Information

13.9% Efficiency Ternary Nonfullerene Organic Solar Cells Featuring Low-structural Order

Baocai Du^{a,b}, Renyong Geng^c, Wei Li^{a,b}, Donghui Li^{a,b}, Yuchao Mao^{a,b}, Mengxue Chen^{a,b}, Xue Zhang^{a,b}, Joel A. Smith^d, Rachel C. Kilbride^d, Mary E. O’Kane^d, Dan Liu^{a,b}, David G. Lidzey^d, Weihua Tang^{c*}, Tao Wang^{a,b,*}

^a School of Materials Science and Engineering, Wuhan University of Technology, Wuhan 430070, China E-mail: twang@whut.edu.cn

^b State Key Laboratory of Silicate Materials for Architectures, Wuhan University of Technology, Wuhan 430070, China

^c School of Chemical Engineering, Nanjing University of Science and Technology, Nanjing 210094, China E-mail: whtang@njust.edu.cn

^d Department of Physics and Astronomy, University of Sheffield, Sheffield, S3 7RH, UK

Materials

m-INPOIC was synthesized as in our previous work.¹ PBDB-T, IT-M were purchased from Solarmer Materials (Beijing) Inc. The molecular weight and polydispersity index of PBDB-T are 11.5K (M_n) and 1.18, respectively. ZnO precursor solution was prepared according to a previous literature report.² The processing solvents used in the fabrication processes were of reagent grade.

Device Fabrication

All organic solar cells were fabricated in an inverted structure. The prepatterned indium tin oxide (ITO)-glass substrates (resistance $\approx 15 \Omega$ per square) were cleaned by sequential sonication in water, ethanol, and isopropyl alcohol for 10 min each, and dried at 100 °C on a hotplate before use. These substrates were further treated with ultraviolet/ozone for 15 min before solution processing. The 30 nm thick ZnO films were spin-coated onto cleaned ITO substrates and then heated at 200 °C for 30 min in air. The photoactive layer solutions were prepared by dissolving the PBDB-T:m-INPOIC:IT-M with the weight ratios of 1:1:0, 1:0.9:0.1, 1:0.8:0.2 in chlorobenzene respectively (20mg/ml with 0.5 vol% 1,8-diiodooctane (DIO)). Subsequently, the prepared blend solutions were spin-coated on ZnO modified ITO substrates at 2200 rpm for 40 s to give the film

with thickness of about 105 nm, in a nitrogen-filled glove box. After the casting of the active layer, all devices were further treated with thermal annealing at 100 °C for 10 min. Then 10 nm MoO₃ and 100 nm Ag were thermally evaporated forming the anode and counter electrode under high vacuum to finish the device preparation. The size of the photoactive area defined by the overlapping of anode and cathode is 4 mm².

Instruments and Characterization

Film thickness was measured using a spectroscopic ellipsometer (J. A. Woollam, USA). The surface morphologies of the active layers were characterized by TEM (JEOL, Japan). GIWAXS was conducted with 10 keV X-rays and an incidence angle of 0.16° using the I07 beamline at Diamond Light Source synchrotron (UK) as part of session SI22651-1. Synchrotron GISAXS measurements were conducted using the beamline BL16B1 at the Shanghai Synchrotron Radiation Facility in China. Film absorption spectra were measured using a UV–visible spectrophotometer (HITACHI, Japan). PL was obtained using a PL microscopic spectrometer (Flex One, Zolix, China) with a 532 nm CW laser as the excitation source. Device J–V characterization was performed under AM 1.5G (100 mW/cm²) illumination using a Newport 3A solar simulator (USA) in air at room temperature. The light intensity was calibrated using a standard silicon reference cell certified by the National Renewable Energy Laboratory (NREL, USA). J-V characteristics were recorded using J-V sweep software developed by Ossila Ltd. (UK) and a Keithley 2612B (USA) source meter unit. EQE was measured with a Zolix (China) EQE system equipped with a standard Si diode. Impedance measurements were performed on an XM-studio electrochemical workstation (Solartron, UK).

Hole-only and electron-only devices were fabricated to measure the hole and electron mobilities of devices using the space charge limited current (SCLC) method with hole-only devices of ITO/PEDOT:PSS/Active layer/MoO₃/Ag and electron-only devices of ITO/ZnO/Active layer/Ca/Ag. The mobilities (μ_h or μ_e) were determined by fitting the dark current to the model of a single carrier SCLC, described by the equation 1:

$$J = \frac{9}{8} \varepsilon_0 \varepsilon_r \mu \frac{V^2}{d^3} \quad (1)$$

Where J is the current, ε_0 is the permittivity of free space, ε_r is the material relative permittivity, d is the thickness of the active layer and V is the effective voltage. The effective voltage can be obtained by subtracting the built-in voltage (V_{bi}) from the applied voltage (V_{appl}), $V = V_{appl} - V_{bi}$. The mobility can be calculated from the slope of the $J^{1/2}$ -V curves.

To quantify and compare the phase separation in the non-fullerene photovoltaic blends, the 1D GISAXS profiles were fitted using a universal model expressed in Equation 2 using the fitting software SASView (Version 3.1.2). The first term of the equation is the so-called Debye–Anderson–Brumberger (DAB) term, where q is the scattering wave vector, A_1 is an independent fitting parameter, and ξ is the average correlation length of the PBDB-T domain. The second term represents the contribution from fractal-like aggregations of m-INPOIC. Here, $P(q, R)$ is the form factor of m-INPOIC. $S(q, R, \eta, D)$ is the fractal structure factor, which describes the interaction between primary particles (defined as 4 nm in our fitting) in this fractal-like aggregation system, with R the mean radius of primary m-INPOIC aggregates, and η the correlation length of the fractal-like structure. The average correlation length of the clustered m-INPOIC phases can be defined by the Guinier radius (R_g) of the network, where $R_g = \sqrt{\frac{D(D+1)}{2}} \eta$.

$$I(q) = \frac{A_1}{[1+(q\xi^2)]^2} + A_2 \langle P(q, R) \rangle S(q, R, \eta, D) + B \quad (2)$$

$$S(q) = 1 + \frac{\sin[(D-1) \tan^{-1}(q\eta)] b \pm \sqrt{b^2 - 4ac}}{(qR)^D} \frac{D\Gamma(D-1)}{\left[1 + \frac{1}{(q\eta)^2}\right]^{(D-1)/2}} \quad (3)$$

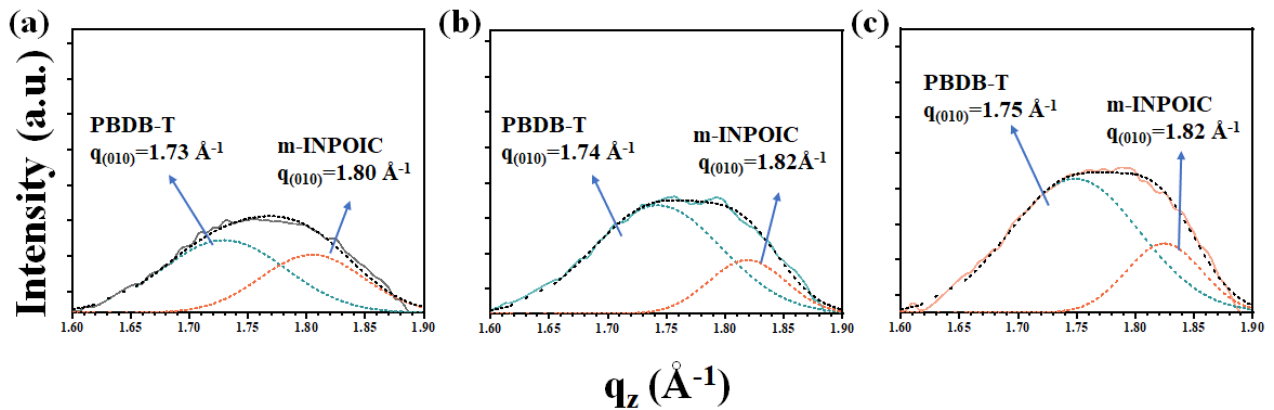


Figure S1. Multi-peak fits of the out-of-plane GIWAXS line cuts at the high q region for the blend films of (a) PBDB-T:m-INPOIC, (b) PBDB-T:m-INPOIC:IT-M (10wt%), (c) PBDB-T:m-INPOIC:IT-M (20 wt%).

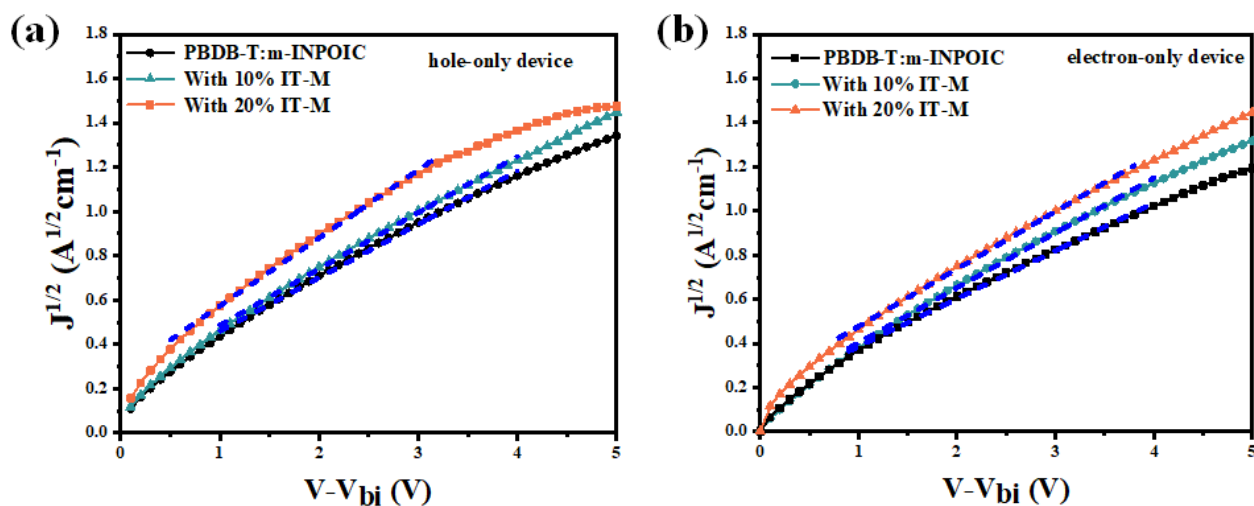


Figure S2. (a) Hole mobility and (b) electron mobility based on PBDB-T:m-INPOIC and its ternary devices with different amounts of IT-M.

Reference

- (1) Feng, H.; Song, X.; Zhang, Z.; Geng, R.; Yu, J.; Yang, L.; Baran, D.; Tang, W. Molecular Orientation Unified Nonfullerene Acceptor Enabling 14% Efficiency As-Cast Organic Solar Cells. *Adv. Funct. Mater.* **2019**, <https://doi.org/10.1002/adfm.201903269>.
- (2) Sun, Y.; Seo, J. H.; Takacs, C. J.; Seifert, J.; Heeger, A. J. Inverted Polymer Solar Cells Integrated with a Low-Temperature-Annealed Sol-Gel-Derived ZnO Film as an Electron Transport Layer. *Adv. Mater.* **2011**, *23*, 1679–1683.